https://doi.org/10.17563/rbav.v38i3.1147

Spinner with fan and Arduino for assembly of organic light emitting diodedevices

Spinner com ventoinha e Arduino para montagem de dispositivos diodos orgânicos emissores de luz

Emerson Roberto Santos[1*], Sidinei dos Santos Sousa[2], Elvo Calixto Burini Junior[3], Roberto Koji Onmori[4], Wang Shu Hui[1]

ABSTRACT

In this work, a spinner apparatus was mounted with some characteristics, such as low cost, easy operation, compact size, easy adaptation into the little glove box systems, no vacuum pump and low maintenance. First, three different fans were analyzed to be used in the spinner apparatus. Then, the Arduino electronic circuit was analyzed and programmed to control the rotation speed using a pulse width modulation (PWM) and steps of acceleration with the signal distortion (caused by pulse width modulation) of the fan intern tachometer. After, the interface between the user and spinner apparatus was performed with information about navigation through the menus, input of process parameters as rotation speed, rotation time, and calibration menu. Successive depositions of organic thin films to assemble organic light emitting diodes (OLED) devices were used with the spinner apparatus. The experiment compared indium tin oxide (ITO) thin film anodes with sheet resistances of 8 and 12 Ω/☐ supplied by different manufacturers in the structure of the OLEDs. Current-voltage (I-V) curves of OLED devices showed that the ITO/glass of 12 Ω/☐ presented better results with low variability and highest current values. All OLED devices presented some luminance showing the efficiency of spinner apparatus.

Keywords: Arduino, spinner, OLED.

RESUMO

Neste trabalho, um aparato spinner foi montado com algumas características, tais como: baixo custo, fácil operação, tamanho compacto e fácil adaptação dentro de sistemas glove boxes pequenas, sem bomba de vácuo e baixa manutenção. Primeiro, três diferentes ventoinhas foram analisadas para serem utilizadas no aparato spinner. Então, o circuito eletrônico Arduino foi analisado e programado para controlar a velocidade de rotação utilizando (PWM) e passos de aceleração com distorção de sinal (causada pela modulação por largura de pulso) do tacômetro interno da ventoinha. Depois, a interface entre o usuário e o aparato spinner foi realizada com informação sobre a navegação através de menus, entrada de parâmetros de processos como velocidade de rotação, tempo de rotação, e menu de calibração. Deposições sucessivas de filmes finos orgânicos para montagem de dispositivos diodos orgânicos emissores de luz (OLEDs) foram utilizados com o aparato spinner. O experimento comparou anodos de filmes finos de óxido de índio e estanho (ITO) com resistências de folha de 8 e 12 Ω/☐ fornecidos por diferentes fabricantes nas estruturas dos OLEDs. Curvas de corrente-tensão (I-V) dos dispositivos OLEDs mostraram que o ITO/vidro de 12 Ω/☐ apresentou melhores resultados com baixa variabilidade e valores de correntes mais altos. Todos os dispositivos OLEDs apresentaram alguma luminância mostrando a eficiência do aparato spinner.

Palavras-chave: Arduino, spinner, OLED.

1.Universidade de São Paulo – Escola Politécnica – Departamento de Engenharia Metalúrgica e de Materiais – São Paulo/SP – Brazil
2.Faculdade de Tecnologia de São Paulo – Departamento de Sistemas Eletrônicos – São Paulo/SP – Brazil
3.Universidade de São Paulo – Instituto de Energia e Ambiente – São Paulo/SP – Brazil
4.Universidade de São Paulo – Escola Politécnica – Engenharia Elétrica – São Paulo/SP – Brazil

Corresponding author: emmowalker@yahoo.com.br

Received: 2020 Jan. 17 **Approved:** 2020 Jan. 30

INTRODUCTION

After decades, light emitting diode (LED) devices have been quickly emerged and applied in almost all sectors of the light market, bringing new concepts, such as energy saving, long lifetime, good efficiency, low voltage, no ballast and wide range of emission colors (compared with other sources of lighting)[1-3]. However, the technology is in constant evolution, then organic light emitting diode (OLED) devices have been developed reaching some properties of LED devices, including other advantages, such as emission on flat surface providing better scattering of light, easy method of fabrication and varied geometries[4-7].

For the assembly of OLED devices, the concept of multilayers created by a technique called spin-coating have been used[8-11]. Spin-coating is widely used to create thin films, not only for OLED devices, but also for organic photovoltaic cell (OPV) devices[12-15]. This technique uses a commercial equipment known as spinner, which has basically controls of rotation speed, rotation time and vacuum (to hold the sample during the rotation process)[16-18]. Organic devices must be mounted inside controlled-atmosphere glove box systems due to degradation effect, caused mainly by oxygen and moisture in organic layers[19-22].

Commercial spinners have robust sizes and connections for the vacuum pump. For this reason, they are difficult to use inside glove box systems, mainly with reduced intern sizes, as showed in Fig. 1.

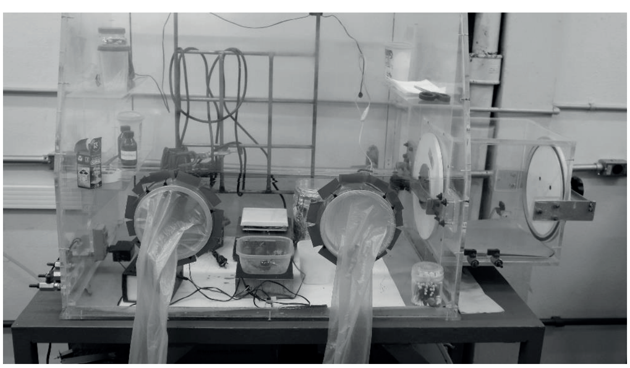

Figure 1: Glove box chamber used to assemble of OLED devices.

In this work, a spinner was mounted using a microcomputer fan and other components with the objective to obtain low cost, easy operation, compact size, easy adaptation into little glove box systems, no vacuum pump and low maintenance. In commercial spinners on the shaft of motor, there is a horizontal surface called chuck, where the blade (glass, in OLED devices) is positioned and held by vacuum pump[23,24]. Organic chemical solution is put on the surface of the blade and the motor is turned on; then the centrifugal force expels off the excess of chemical solution on the blade forming a thin film[25]. Figure 2 shows the complete mechanism used in the spin-coating technique.

The suggested spinner apparatus must have similar method of operation compared with commercial equipment, which have different prices, however, this equipment have other characteristics, such as manufacturer's guarantee, large case with lid, high torque motor, and large range for rotation speed. Some models also have ramps with acceleration and deceleration speeds.

The proposed spinner apparatus was mounted with low cost and with very simple and easy-to-be-found components. Although, it is not equipped like most commercial equipment, the apparatus is capable of assembling OLED devices with good quality in terms of electrical and optical characteristics compared with devices mounted by commercial equipment. The mean cost of commercial equipment represents hundred times higher than the proposed spinner apparatus.

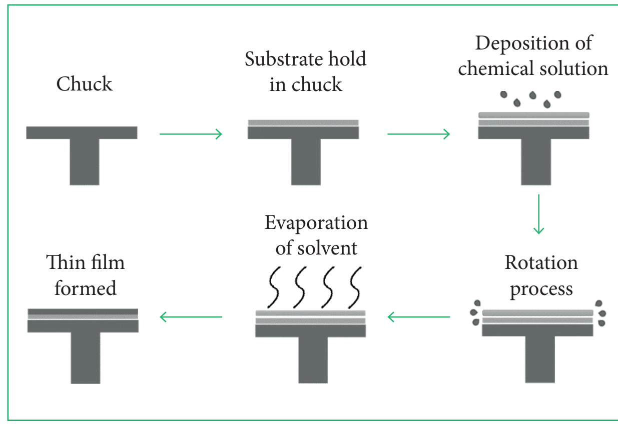

Figure 2: Complete mechanism of spin-coating technique.

The OLED devices have been mounted with a few thin films forming a multilayer structure: (1) transparent conductive oxide (TCO) as anode and deposited on glass substrates (both generally commercial); (2) chemical solution of polymeric material, named hole transport layer (HTL); (3) chemical solution of organic material to emission of light; (4) chemical solution of organic material, named electron transport layer (ETL); and (5) metal as cathode deposited on top[26,27]. Figure 3 shows this OLED device structure.

The devices must be encapsulated to avoid OLEDs degradation (such as elevation of threshold voltage and decreasing of light emission)[28-30].

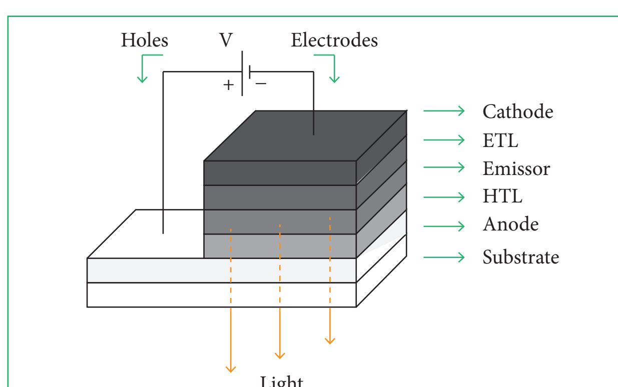

Figure 3: OLED device structure formed with the deposition of successive organic thin films.

A very important aspect to be considered in the assembly of OLED devices is related to the thickness for each layer deposited. If the layer thickness is too thin, a short circuit may occur damaging the device, and if the thickness layer is too thick, the device will emit a considerable part of its energy received from source power in heat form.

Nonsmooth surface may generate other problems, such as unbalancing of the charge carriers, or even creation of trapped charges decreasing considerably the devices performance[31,32]. Therefore, complete control of the thickness is necessary for each organic thin film formed.

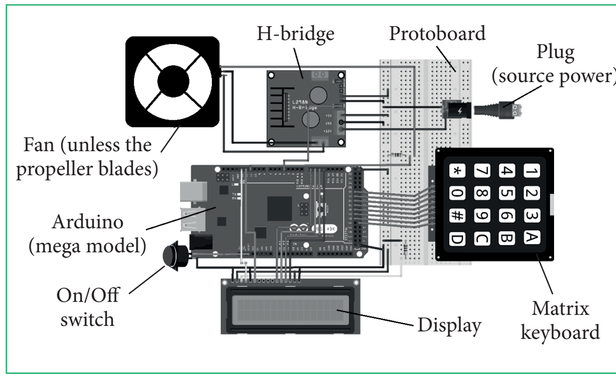

Figure 4: Complete electrical circuit mounting diagram.

MATERIAL AND METHODS

The components used in tests and assembly of spinner apparatus were: (1) Arduino electronic circuit, Mega model used to control data processing; (2) Arduino software open source, version 1.8.6; (3) driver motor DC/step, L298N model used to control of fan rotation; (4) matrix keyboard used to type the process parameters, such as rotation and time values; (5) liquid crystal display (LCD) with 2 lines × 16 columns used to visualize process parameters; (6) source power (Sunny company) with automatic input voltage of 110 or 220 V and output of 12 V and 2 A with P4 cord connection; (7) digital laser tachometer (Minipa, model MDT-2238A) used to analyze rotation fans; (8) digital oscilloscope (Minipa, model MO-2061) used in the study of the electrical signals generated by sensors and Arduino electronic circuit; (9) plastic case necessary to store the Arduino, keyboard and display of spinner apparatus and (10) three fans (with intern tachometer using the third cord available).

The propeller blades of all fans were removed (resting the plastic part plane on center): fan A (Viper Company) measuring 0.12 × 0.12 m; fan B measuring 0.08 × 0.08 m and fan C measuring 0.12 × 0.12 m.

Arrangement of Arduino electronic circuit

There are two class in the Arduino electronic circuit (Mega model): the digital pins (numbered from 0 to 54) to be used in the 0 logic level (corresponding to 0 V) or 1 logic level (corresponding to 5 V) and the analog pins (numbered from 0 to 15) with operation range from 0 to 5 V. The total of 17 pins were applied to use all components in the Arduino: (a) 6 pins to operate the LCD display (pins: 13, 12, 14, 15, 16 and 17); (b) 1 pin to control the pulse weight modulation (PWM) (pin: 4); (c) 1 pin to extract the rotation (pin: 11); (d) 1 pin to reset the spinner apparatus (pin: reset); and (e) 8 pins to the matrix keyboard (pins: 30, 32, 34, 36, 38, 40, 42 and 45). Figure 4 shows the complete electrical scheme of the mounted circuit.

Speed and rotation time controls

Pulse weight modulation of the electronic circuit was used to control the rotation speed[33]. This electronic circuit is based on pulse control duration, which is used with the H-bridge promoting the rotation control (no change in the torque motor). Before the speed analyses, it is necessary to know previously the rotation per minute (rpm) value to control the motor speed by PWM[34]. In this case, the fan intern tachometer was used to measure its rotation and also to correct the speed in real time. The advantage to use its intern tachometer is the actualization rate, because the sensor generates an electrical pulse by half rotation. Arduino has a function to measure individually the time for each pulse with resolution up to 3 μs pulse In to obtain very speed measurements per second[35].The electrical signal generated by the fan represents a square wave, since the signal is generated for each half rotation using a constant value of 30,000 and divided by the tachometer signal period of 6.98 ms, resulting in a rotation speed of 4,297 rpm.

PWM control to rotation speed reading

In the reading of electrical signal obtained by the fan tachometer, it was verified that an alteration of PWM value causes distortion in the electrical signal received from the fan. This process may generate inaccurate results in the measurements of rotation. This distortion is probably caused by the principle of switching the PWM on and off several times per second and the fact that the tachometer is operated by the same pin used for the PWM control. So, a simple algorithm was implemented to solve this distortion trouble avoiding variations in the rotation speed measured by Arduino. Because this distortion has very short duration, the PWM discards any measurement value below 0.1 milliseconds.

Fan acceleration and speed adjustment

In order to have the shortest acceleration time, a process with two acceleration phases was proposed.

The first stage has a simple algorithm, at the beginning of rotation process, the fan reaches 255 level of PWM to maximum acceleration. When the measured rotation is equal or greater than 90% of the required rotation by user, the spinner apparatus begins the second stage. This second stage of acceleration is used to adjust the curve used to prevent the PWM value for any rotation using a mathematics function.

When leaving the first stage, the fan will be close to the rotation value required by the user with maximum acceleration (PWM = 255). Figure 5 shows the PWM level vs. rotation speed measured.

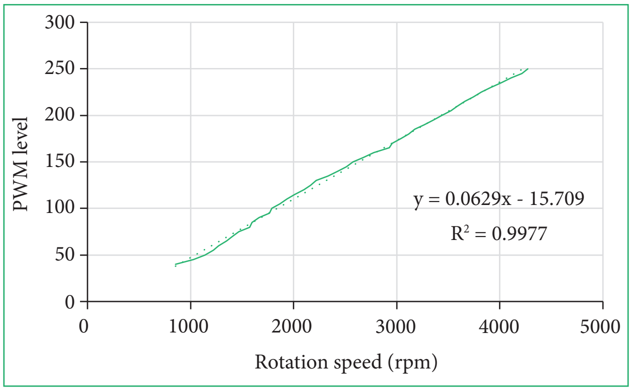

Figure 5: PWM level vs. rotation speed measured.

As observed in Fig. 5, both the fan rotation and PWM level have a linear relationship, then it is possible to use the least squares method (LSM) to calculate the straight line of equation.

However, different fans will have different maximum speeds and it is possible that the same fan presents variations on its maximum rotation by elapsed time, due to variable factors. For this reason, an algorithm using LSM was implemented to calculate the relation for PWM vs. rotation speed required by user with the calibration of the straight line of equation.

In order to validate the linear regression of the spinner apparatus in comparison with Microsoft Excel software, two methods were used to calculate the straight line of equation by LSM generating some results with the same equations to calculate the R^2, that is a statistical variable of quality for this method, where R^2 is most near to 1, corresponding to the better value, as showed in Table 1.

Table 1: PWM level measured vs. PWM level calculated.

	Equation	R^2
Spinner	rpm = 0.063 × PWM –15.71	0.9977
Excel	rpm = 0.063 × PWM – 15.71	0.9977

Table 1 reveals that the spinner apparatus is capable to perform the linear regression by LSM in the same way when compared with the Microsoft Excel software, validating calibration. After obtaining the calculated linear regression, an algorithm was implemented for the spinner apparatus to save the information of linear equation in EEPROM memory of Arduino electronic circuit allowing the use of these data in the next initialization of the apparatus (unnecessary new calibration)[36].

Interface

The spinner apparatus has an intern program to control the values typed by the user, such as rotation speed in rpm and rotation time in seconds. Figure 6 presents the complete steps showed in the display before the rotation process. In the initial process of rotation, the spinner apparatus will renovate the values of rotation speed in real time, then the difference percentage obtained between the actual rotation and the required by the user is showed on display and the remaining rotation time in seconds. After the elapsed time, the fan is automatic turned-off and the initial information returns to the display.

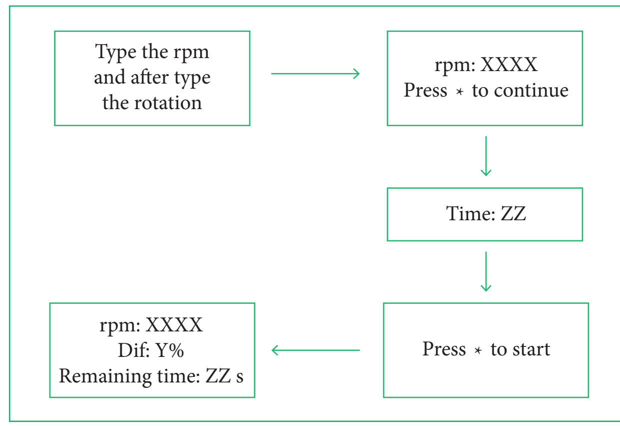

Figure 6: Steps showed by display for complete rotation process.

Display interface

For better convenience, the most commonly used shortcut keys for depositing thin films in the laboratory with preset speed and rotation time values have been implemented: A – corresponding to 3,000 rpm per 60 s, B – corresponding to 2,500 rpm per 60 s, and C – corresponding to 2,000 rpm per 60 s.

Calibration interface on display

The D key is used to access the spinner calibration mode. When pressed, the spinner will require the value of the limit rotation, because the apparatus will calculate the maximum rotation obtained by the fan with the linear equation. After, a message shows the confirmation of the limit rotation selected and the calibration process is started indicating the rpm and PWM values measured in real time on display.

After collecting all data, the spinner apparatus will calculate the linear regression by LSM and show the stable values of the equation on display. Then, the spinner apparatus is automatically

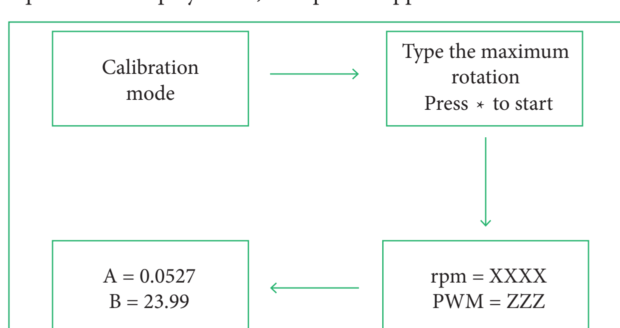

Figure 7: Steps showed on display for calibration interface.

restarted returning to the initial information. The complete calibration method is showed in Fig. 7. The program of Arduino electronic circuit used in this spinner apparatus is available in the website[37].

Assembly and analyses of OLED devices

OLED devices were assembled with the following structure:

a. Electrode anodes of indium tin oxide (ITO) thin films deposited on glass substrates with 8 Ω/□ (Displaytech) and 12 Ω/□ (Diamond Coatings), and cut in geometry of 0.025 × 0.025 m. Then, four stripes were formed with the ITO thin films using: hydrochloric acid, zinc powder, cotton and Magic tape (Scotch 3M) to the masking of region preserved. After that, the samples were cleaned using two processes: current water and domestic neutral detergent and surgical gloves rubbing the surfaces of the ITO thin films and some drops of Aqua Brilho (Adespec) were put on the ITO thin films and rubbed with cotton until the complete elimination of commercial product.
b. Deposition (using the spinner apparatus) of PEDOT:PSS (as HTL supplied by Sigma-Aldrich) at 3,000 rpm per 60 s forming a thin layer, which was dried at 333.15 K per 300 s. To hold the sample on the "chuck" of the spinner apparatus, a double-sided tape was used.
c. PVK (Sigma-Aldrich) polymer (as emitting material) was diluted in 1,2,4-trichlorobenzene (Tedia) with 10 mg mL^{-1} concentration deposited at 3,000 rpm per 60 s, forming a thin layer, which was dried at 333.15 K per 300 s.
d. Alq_3 (as ETL) synthesized at laboratory, which was thermally evaporated.
e. Thermally evaporation of electrode cathode formed with aluminum (Balzers) thin film on top.

Four OLED devices were obtained on each sample mounted at the same time with active area of 0.003 × 0.003 m. The devices were polarized using a power source (Keithley, model 2400), that was used to apply the voltage and to collect the electrical current.

RESULTS AND DISCUSSION

Before the spinner apparatus assembly, three fans were polarized at 12 V and the rotation speeds were analyzed. The results revealed highest speed for B fan reaching 4,343 rpm with high stability. Table 2 shows the analyses for all fans measured and reveals that fan A had bad performance and lowest rotation speed with high standard deviation obtained.

For the assembly of OLED devices a rotation speed of 3,000 rpm was used for the deposition of organic layers, then the fan C was discarded to the assembly of spinner apparatus.

In order to have reliability of the intern tachometer measurements, it is necessary to compare it with a commercial tachometer. In this case, a commercial tachometer MDT-2238A (Minipa) was used. The criterion used in these analyses was the comparison of the average rotation with the standard deviation measured for some rotation speeds comparing the commercial tachometer and the fan B intern tachometer, as showed in Table 3.

Table 3 shows near values of different rotation speeds for both methods compared. Low variations were obtained, if compared with the rotation speed required, mainly to the intern tachometer, but the fan B still revealed reliability to assemble thin films used in the assembly of OLED devices. The analysis of the rotation speed process is very promising and it shows the elapsed time of 1 s to reach the required rotation speed and 3 s to stabilize the speed rotation required by user for each different rotation speed analyzed, as showed in Fig. 8.

Table 2: Performance for all fans polarized at 12 V.

Fans	Maximum Rotation Speed (rpm ± standard deviation)
A	2,330 ± 13
B	4,343 ± 3
C	2,640 ± 1

Table 3: Comparison of commercial tachometer and intern tachometer of fan B for different rotation speeds.

Rotations required by user	Commercial tachometer rotation measured average (± standard deviation)	Intern tachometer – fan B Measured rotation Average (± standard deviation)
3,000	3,073 (± 20)	3,023 (± 44)
2,500	2,584 (± 16)	2,510 (± 30)
2,000	2,110 (± 23)	2,023 (± 35)
1,500	1,590 (± 14)	1,508 (± 14)

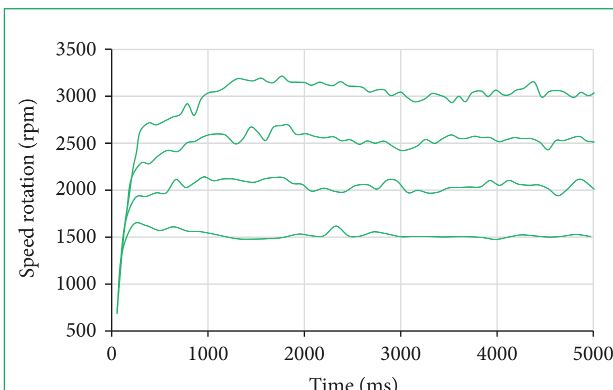

Figure 8: Speed rotations vs. time measurements for the spinner apparatus with fan B.

OLED devices were mounted with ITO/glass anodes using different sheet resistances and manufactures with 8 and 12Ω/□. The I-V curves of OLEDs with ITO/glass of 8 Ω/□ clearly showed the electrical behavior of diode as expected for these devices, but A low variation of the I-V curves was observed in the results revealing possible variations in the quality of the electrode anodes (such as different: thickness, surface roughness and morphology of ITO thin films).

The OLED devices mounted with ITO/glass anodes of 12 Ω/☐ showed the better reproducibility of I-V results obtaining, practically, a superposition of the diode curves with highest levels of electrical current.

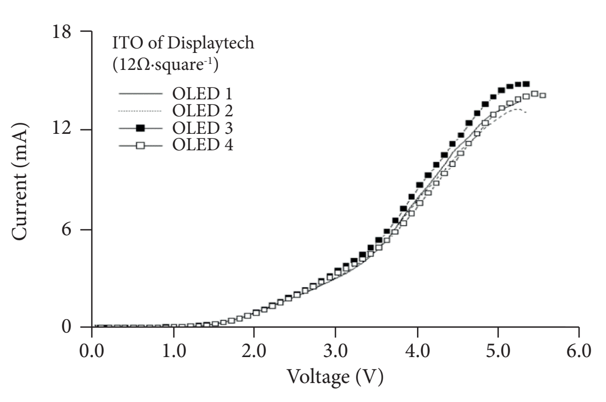

Figure 9: I-V curves of four OLED devices mounted at the same time with ITO/glass of 12 Ω/☐.

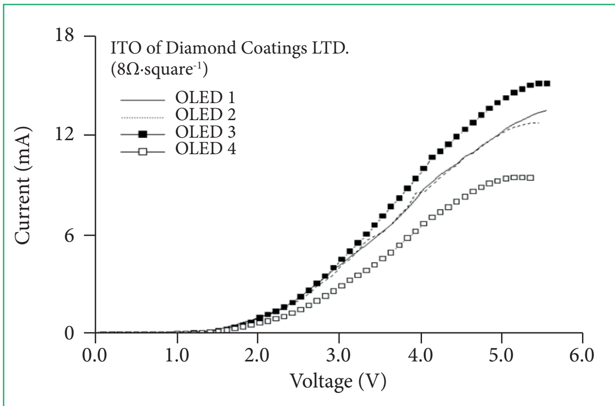

Figure 10: I-V curves of four OLED devices mounted at the same time with ITO/glass of 8 Ω/☐.

All devices presented some luminance as showed in Fig. 11 for the OLED mounted with the ITO/glass of 12 Ω/☐ and active area of ≈3.0 × 3.0 mm with four OLED devices mounted on the geometry of ≈25.0 × 25.0 mm for each blade. In other work, the same structures of OLED devices were mounted and analyzed showing the efficiency of this spinner apparatus[38].

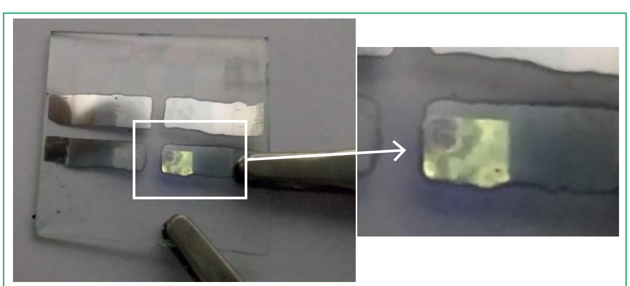

Figure 11: Light emission of OLED device mounted with spinner apparatus using ITO/glass of 12 Ω/☐

CONCLUSION

The development of a low-cost spinner apparatus mounted (US$ 37.27) with a microcomputer fan, Arduino electronic circuit and few components presented good results, such as easy operation, compact size, easy adaptation into the little glove box systems, no vacuum pump and low maintenance. Precise results were obtained by the fan intern tachometer, moreover it allowed the connection compatible with the Arduino. The PWM had precise performance to maintain stable rotation of fan by elapsed time. The use of a fan connected with the interface of Arduino (Mega model) to send/receive data, the keyboard to type the process parameters and the LCD display to exhibition of process parameters values facilitated its use.

The spinner apparatus mounted successive organic thin films in the structure of OLED devices using glass/ITO/PEDOT:PSS/Alq_3/Al with ITO/glass thin films of different sheet resistances of 8 and 12 Ω/☐. Four OLED devices for each ITO/glass were mounted at the same time and analyzed revealing similar aspect of diode curve with some luminance in the devices, but better performance was pronounced for the ITO/glass of 12 Ω/☐ presenting low variation and elevation of electrical current.

ACKNOWLEDGMENTS

The authors thank the financial support from the Brazilian agency Coordenação de Aperfeiçoamento de Pessoal de Nível Superior (CAPES) by post-doctoral scholarship. They thank also the Escola Politécnica da Universidade de São Paulo, Engenharia Metalúrgica e de Materiais, Laboratório de Engenharia de Macromoléculas by materials, equipments and installations.

REFERENCES

1. Gupta SD. Light Emitting Diodes for Agriculture. Singapore: Springer Nature. 2017. https://doi.org/10.1007/978-981-10-5807-3

2. Tin PT, Nhan NHK, Minh THQ, Nguyen TN, Voznak V, Trang TT. Sr2Si5N8:Eu2+ phosphor: a novel recommendation for improving the lighting performance of the 7000 K remote-packaging white LEDs. P Est Acad Sci. 2018;67(4):337-41. https://doi.org/10.3176/proc.2018.4.06

3. Garcia-Caparros P, Chica RM, Almansa EM, Rull A, Rivas LA, García-Buendía A, et al. Comparisons of different lighting systems for horticultural seedling production aimed at energy saving. Sustainability. 2018;10(9):3351-67. https://doi.org/10.3390/su10093351

4. Cheng T-Y, Lee J-H, Chen C-H, Chen P-H, Wang P-S, Lin C-E, et al. Carrier Transport and Recombination Mechanism in Blue Phosphorescent Organic Light-Emitting Diode with Hosts Consisting of Cabazole- and Triazole-Moiety. Sci Rep. 2019;9(3654):1-12. https://doi.org/10.1038/s41598-019-40068-w

5. Liou JJ, Chen W-R, Kang C-C, Lee K-W, Feng S-W, Huang C-J. White Organic Light-emitting Diode Using Nano-double Ultrathin Carrier-trapping Materials in Performance Stability. Sensor Mater. 2019;31(1):131-9. https://doi.org/10.18494/SAM.2019.1995

6. Cebrián C, Mauro M. Recent advances in phosphorescent platinum complexes for organic light-emitting diodes. Beilstein J Org Chem. 2018;14:1459-81. https://doi.org/10.3762/bjoc.14.124

7. Mazumder MAJ, Heather Sheardown H, Amir Al-Ahmed A. Functional Polymers, Switzerland: Springer Nature; 2019.

8. Banerji A, Kirchmeyer S, Meerholz K, Scharinger F. Teaching Organic Electronics - Part II: Quick & Easy Synthesis of the (Semi-)Conductive Polymer PEDOT: PSS in a Snap-Cap Vial. World J Chem Educ. 2019;7(2):166-71. https://doi.org/10.12691/wjce-7-2-16

9. Han YW, Song HJ, Jeon SJ, Lee HS, Ko EJ, Song CE, et. al. Excellent carrier transport materials produced by controlled molecular stacking and their application in flexible organic electronic devices. J Mater Chem A. 2019;7(24):14790-805. https://doi.org/10.1039/c9ta02213a

10. Liou JJ, Hsu P-H, Chen W-R, Chou D-W, Lee K-W, Wang N-F. et al. Improving the Quality and Electrical Properties of Poly(3,4-ethyl enedioxythiophene):Poly(styrenesulfonate) (PEDOT:PSS) Film by Heating and Stirring the Solution. Sensor Mater. 2019;31(1):211-9. https://doi.org/10.18494/SAM.2019.2116

11. Liou J-H, Hsu P-F, Chen Y. Hole-Buffer Material Derived from Pyrene, Schiff Base and Tris to Enhance Emission Efficiency of Polymer Light-Emitting Diodes. Journal of Materials Science and Chemical Engineering. 2018;6(3):31-46. https://doi.org/10.4236/msce.2018.63003

12. Li X, Pan F, Sun C, Zhang M, Wang Z, Du J, et al. Simplified synthetic routes for low cost and high photovoltaic performance n-type organic semiconductor acceptors. Nat Commun. 2019;10(519):1-11. https://doi.org/10.1038/s41467-019-08508-3

13. Webb GA. Modern Magnetic Resonance. Switzerland: Springer Nature; 2019.

14. Mahesh K, Karpagam S, Goubard F. Conductive and photoactive nature of conjugated polymerbased on thiophene functionalized thiazole orbenzothiadiazole. Express Polym Lett. 2018;12(3):238-55. https://doi.org/10.3144/expresspolymlett.2018.22

15. Hofmann M, Aydogan C, Lenk C, Krivoshapkina Y, Lenk S, Volland B, et al. Selective Pattern Transfer of Nano-Scale Features Generated by FE-SPL in 10 nm Thick Resist Layers. American Journal of Nano Research and Applications. 2018;6(1):11-20. https://doi.org/10.11648/j.nano.20180601.12

16. Belous A, Tovstolytkin A, Solopan S, Shlapa Y, Fedorchuk O. Synthesis, Properties and Applications of some Magnetic Oxide Based Nanoparticles and Films. Acta Phys Pol A. 2018;133(4):1006-12. https://doi.org/10.12693/APhysPolA.133.1006

17. McGraw JD, Fowler PD, Ferrari ML, Dalnoki-Veress K. Relaxation of non-equilibrium entanglement networks in thinpolymer films. Eur Phys J E. 2013;36(7):1-8. https://doi.org/10.1140/epje/i2013-13007-2

18. 18. Manikandan NS, Shanthi B, Muruganand S. Construction of spin coating machine controlled by arm processor for physical studies of PVA. Int J Electron Electr Eng. 2015;3(4):318-22. https://doi.org/10.12720/ijeee.3.4.318-322

19. 19. Pal AJ. Solar module installation in India: concerns options and roadmap. Curr Sci. 2019;116(5):714-22. http://doi.org/10.18520/cs/v116/i5/714-722

20. Adachi C, Hattori R, Kaji H, Tsujimura T. Handbook of organic light-emitting diodes. Tokyo: Springer; 2018.

21. Kumar S, Katiyar M. Thin film encapsulation at low temperature using combination of inorganic dyad layersand spray coated organic layer. JEAS. 2017;7(4):140-8. https://doi.org/10.4236/jeas.2017.74011

22. Sun L, Kurosawa Y, Ito H, Makishima Y, Kita H, Yoshida T, et al. Solution processing of alternating PDMS/SiOx multilayer for encapsulation of organic light emitting diodes. Org Electron. 2019;64:176-80. https://doi.org/10.1016/j.orgel.2018.10.027

23. Tyona MD. A theoritical study on spin coating technique. Adv Mater Res. 2013;2(4):195-208. https://doi.org/10.12989/amr.2013.2.4.195

24. Tay FEH. Materials & Process Integration for MEMS. New York: Springer US; 2002. https://doi.org/10.1007/978-1-4757-5791-0

25. Santos ER, Takahashi CM, Takimoto HG, Yoshida S, Oide MT, Burini Junior EC, et al. Low cost spinner developed for deposition of thin films used in OLED devices. Rev Bras Apl Vac. 2018;37(3):87-94. https://doi.org/10.17563/rbav.v37i2.1071

26. Santos ER, Ono ETY, Yoshida S, Oide MYT, Burini Junior EC, Onmori RK, et al. Thin films of zinc oxide doped with aluminium (AZO) used in OLED device structures. Rev Bras Apl Vac. 2018;37(3):139-44. https://doi.org/10.17563/rbav.v37i3.1081

27. Santos ER, Silva ANR, Ono ETY, Yoshida S, Oide MYT, Burini Junior EC, et al. Bulb used as encapsulation method for OLED devices. Rev Bras Apl Vac. 2018;37(2):95-9. https://doi.org/10.17563/rbav.v37i2.1082

28. Santos ER, Moraes JIB, Takahashi CM, Sonnenberg V, Burini EC, Yoshida S, et al. Low cost UV-Ozone reactor mounted for treatment of electrode anodes used in P-OLEDs devices. Polímeros. 2016;26(3)236-41. http://doi.org/10.1590/0104-1428.2257

29. Furukawa T, Nakanotani H, Inoue M, Adachi C. Dual enhancement of electroluminescence efficiency and operational stability by rapid up conversion of triplet excitons in OLEDs. Sci Rep. 2015;5(8429):1-8. http://doi.org/10.1038/srep08429

30. Wu J, Fei F, Wei C, Chen X, Nie S, Zhang D, et al. Cui, Efficient multi-barrier thin film encapsulation of OLED using alternating Al2O3 and polymer layers. RSC Adv. 2018;8(11):5721-7. http://doi.org/10.1039/c8ra00023a

31. Xing X, Lin T, Hu Y-X, Sun Y-L, Mu W-Y, Du Z-Z, et al. Inkjet printing high luminance phosphorescent OLED based on m-MTDATA:TPBi host. Mod Phys Lett B. 2019;33(12):1950149-1-9. https://doi.org/10.1142/S0217984919501495

32. Sun Y, Jiang Y, Sun XW, Zhang S, Chen S. Beyond OLED: efficient quantum dot light-emitting diodes for display and lighting application. Chem Rec. 2019;19(8):1729-52. https://doi.org/10.1002/tcr.201800191

33. Braga NC. Controle PWM de Motor DC (MEC139). Instituto NCB [Internet]. [cited 2019 Dez. 02]. Available at: http://www.newtoncbraga.com.br/index.php/robotica/5534-mec139

34. Vertulo R. Controle de velocidade de Motor CC com Arduino. Electronic Laboratory [Internet]. 2013 [cited 2019 Dez. 02]. Available at: http://labdeeletronica.com.br/controle-de-velocidade-motor-cc/

35. Gantt C. Reading PC Fan RPM with an Arduino. The Makers Wirkbench [Internet]. 2012 [cited 2019 Sep. 18]. Available at: http://themakersworkbench.com/content/tutorial/reading-pc-fan-rpm-arduino

36. Arduino. EEPROM Library [Internet]. 2019 [cited 2019 Sep. 18]. Available at: https://www.arduino.cc/en/Reference/EEPROM/

37. Github. Programation structure used in the Arduino. [Internet]. [cited 2019 Dez. 02]. Available at: Segue o link: https://github.com/kamael251/Spinner/blob/master/Prog_05_01_19_MMQ.ino

38. Füllenbach TC. Estudo de diferentes TCOs utilizados como eletrodos anodos em dispositivo OLEDs. Undergraduate Thesis [Bachelor in Microelectronic Technology]. São Paulo (SP): FATEC-SP; 2019.